AIAA JOURNAL
Vol. 43, No. 7, July 2005

Density Measurements in an Axisymmetric Underexpanded Jet by Background-Oriented Schlieren Technique

L. Venkatakrishnan*
National Aerospace Laboratories, Bangalore 560 017, India

The background-oriented schlieren (BOS) technique has been applied to obtain the mean density field of a complex underexpanded jet flow. The measurements were made on an axisymmetric sonic jet operating at ideally expanded and highly underexpanded values of nozzle pressure ratios. The methodology involved two steps: validation of the filtered backprojection tomography used here, by making measurements on a four-jet configuration followed by density measurements on axisymmetric sonic jets. Pitot measurements made on an ideally expanded sonic jet were utilized for validation of BOS. The presented density fields show that meaningful quantitative data can be extracted by using minimal hardware with this technology.

Nomenclature

D	=	nozzle exit diameter, mm
M_j	=	jet exit Mach number
P_a	=	ambient pressure
P_e	=	jet exit pressure
P_{oj}	=	jet total pressure
x	=	streamwise direction
y	=	vertical direction
z	=	direction along the line of sight of the camera
$\partial\rho/\partial y$	=	density gradient in the vertical plane
θ	=	azimuthal angle of imaging around jet
ρ	=	density
ρ_a	=	ambient density
ρ_e	=	density at nozzle exit

I. Introduction

DEVELOPMENT of new flow diagnostic tools that are nonintrusive and quantitative, as well as applicable to real-life full-scale flows, is an important area of experimental aerodynamics research. Although all optical techniques to study density fields in transparent media (usually gases or liquids) depend on variation of the index of refraction in the medium and the resulting effects on a light beam passing through the test region, quite different quantities are measured with each one. Techniques like schlieren and shadowgraphy provide qualitative information on first and second derivatives of density, respectively. Interferometry, on the other hand, provides quantitative information on the density field, but setting up such instrumentation requires tremendous care.

The choice of lasers as a source of illumination, improvements in charge-coupled device technology, and fast computers for image acquisition and analysis has resulted in a resurgence of quantitative optical methods. A technique proposed by Meier[1,2] called the background-oriented schlieren (BOS), which is a quantitative schlieren technique, is based on the principle that the image of an object is the convolution of the object function and the transfer channel function. Thus, deconvolution will describe the transfer channel function if the object and image are given. A major advantage of this technique is that it requires only a digital still camera with adequate resolution and an appropriate background.

Presented as Paper 2004-2603 at the AIAA 24th Aerodynamic Measurement Technology and Ground Testing Conference, Portland, OR, 28 June–1 July 2004; received 4 August 2004; revision received 25 December 2004; accepted for publication 25 January 2005.

*Scientist, Experimental Aerodynamics Division. Member AIAA.

Earlier studies[2–4] have qualitatively demonstrated several possible applications of BOS; these include density fields of helicopter-generated vortices and supersonic jets. In recent years, there have been some attempts to quantify the density or density gradient field by broadly using the schlieren principle. Prominent among these include the "synthetic schlieren" method proposed by Dalziel et al.,[5,6] which is applied[7] to an oscillating sphere in a stratified flow and agrees very well with theoretical values.[8] The technique implemented here differs from the aforementioned method in the filtered backprojection tomography (FBPT) technique, which does not need assumption of axisymmetry and obtains the density field instead of wave amplitudes.

The first quantitative validation of BOS for obtaining the density field was reported by Venkatakrishnan and Meier.[9] Their BOS data reduction procedure involved three major steps[9]: 1) obtaining the displacements of a structured background in the absence and presence of a flow, 2) calculation of the projected data set in one direction by solving a field equation formed using step 1, and 3) obtaining the density field in one plane using FBPT. They demonstrated excellent agreement of the density field obtained by applying the BOS technique on a cone-cylinder flow at Mach 2.0 (results available in cone tables[10]); separate validation of the tomographic algorithm was found unnecessary because of the excellent agreement with data from the literature.

The present work is a logical extension of application of the BOS technique to a more complex flow, such as an underexpanded axisymmetric sonic jet flow at high speeds ($M_j = 1$). However, to ensure that the extracted plane of interest is indeed passing through the jet center, a validation of the tomographic algorithm is required. This essentially involves two major steps. First, we validate the tomographic technique by applying BOS to extract the central plane of a supersonic multijet flow in a four-jet cruciform configuration. Extraction of the central plane yielding the correct jet physical diameters and spacing would provide adequate confidence in the determination of the density field of the axisymmetric jet in a diametral plane. In the second step, BOS measurements are made in the axisymmetric jet and the density field in a diametral plane is determined by FBPT. This is initially performed on an ideally expanded sonic jet and the extracted centerline values are compared against those calculated from pitot probe measurements on the same jet. The ideally expanded sonic jet is chosen for validation because the absence of shocks makes for easy comparison against conventional pitot data. Thereafter, the technique is applied on a highly underexpanded jet to obtain the density distribution in the central plane.

II. Background-Oriented Schlieren Methodology

The principle of the technique is the refractive index variation due to density gradients. Two images of a deliberately structured background (usually a dot pattern) are obtained. The first is through

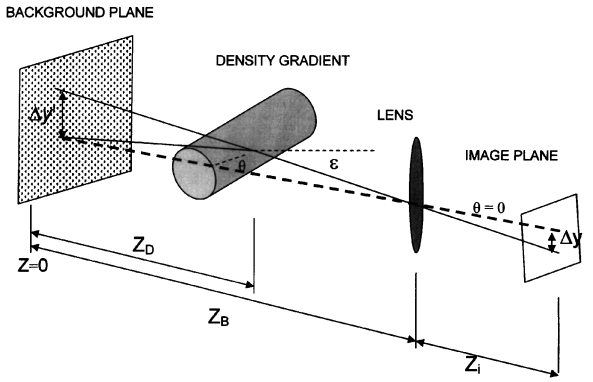

Fig. 1 Optical path for density gradient measurements by light deflection.[1]

the undisturbed transfer channel and the second is through the phase object of interest. The field gradients in the path of the imaging rays cause the deflection of the light rays, leading to shifts in the imaged background. This displacement provides information about the phase object (Fig. 1).

The determination of the density field using BOS thus involves the following steps:

1) Displacements are calculated in the background, which is imaged through the flow of interest. This is done through a particle image velocimetry–type (in-house) cross-correlation algorithm. These displacements are the vectors indicative of density gradient at each point.

2) The line-of-sight integrated density field is calculated by solution of the Poisson equation, which is the gradient of the preceding displacements.

3) Optical tomography (filtered backprojection) is used to determine the density field in the actual plane of interest.

Although a simple Abel inversion method would technically suffice in the case of an axisymmetric flow, Venkatakrishnan and Meier[9] have shown that the method is noise prone. The FBPT would have the further attraction of being universally applicable to axisymmetric and nonaxisymmetric flows. FBPT is based on the principle that, when a field cannot be approximated as two-dimensional in the line of sight, tomography can be used to reconstruct any plane of the field from a set of projections. The tomographic method can be of the transformation, series expansion, or optimization type.[11] Where optical access to the flow is not restricted and several views are available, the first method is the most optimal and is used here. Further details of the BOS technique and its validation can be found in Ref. 9.

III. Experiments

A. Experiments to Validate the Tomographic Technique

The experiments were carried out in the 0.5-m base flow facility wind tunnel at National Aerospace Laboratories (NAL) (Fig. 2). This facility has a moving nozzle around a center body that can provide a supersonic jet flow or multiple jets of desired Mach number (for details see Ref. 12). The experimental program essentially involved two major steps. First, experiments were carried out on a four-jet configuration[13] to validate the tomographic technique. Four identical jets designed for $M_j = 2.5$, with 36-mm exit diameter in a cruciform configuration (two jets each, on the horizontal and vertical planes), made up the multijet afterbody, which was fixed to the centerbody of the tunnel (Fig. 3). The separation between jets at the exit plane along the diameter was 20 mm. As can be expected, obtaining conventional schlieren images of the central vertical plane (section *AA* in Fig. 3b) of the multijet body is difficult in view of the two neighboring jets. The tomographic technique is validated when the reconstructed vertical plane *AA* of the central jets matches the geometric separation distances. The jets were run at an underexpanded condition of $P_{oj}/P_a = 7$ ($P_e/P_a = 5.32$).

B. Experiments on the Underexpanded Axisymmetric Sonic Jet

In the second step, experiments were carried out on an axisymmetric jet issuing from a convergent nozzle at Mach 1.0. BOS measure-

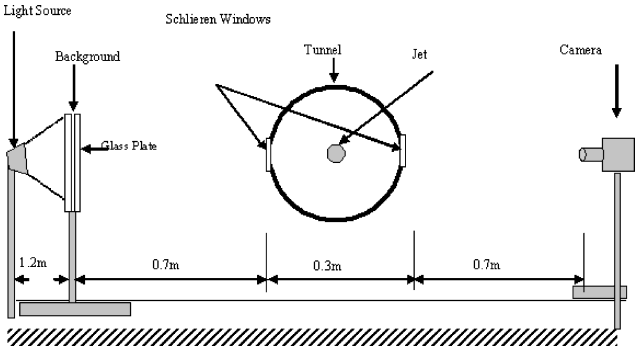

Fig. 2 Schematic of experimental setup.

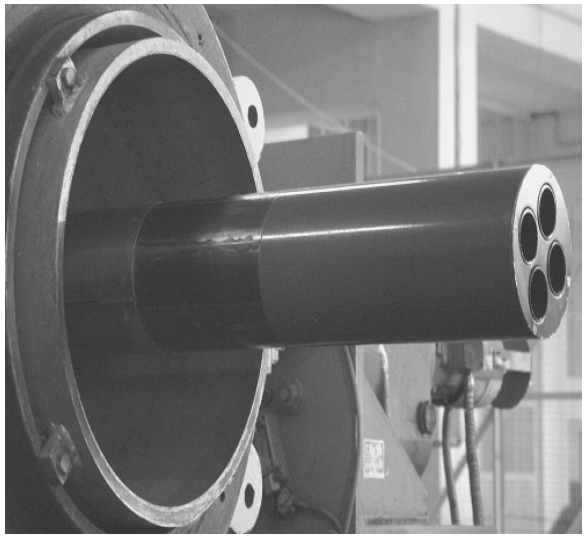

a)

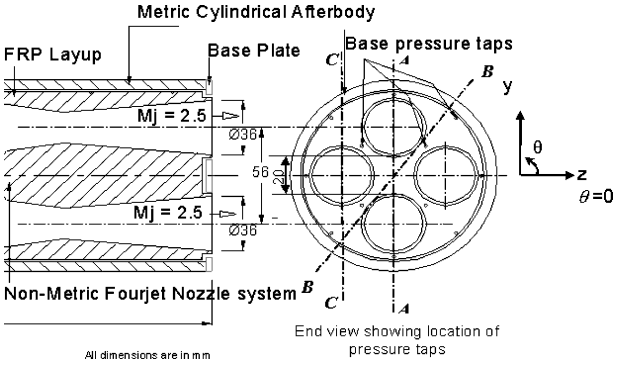

b)

Fig. 3 Multijet in the NAL Base Flow facility.

ments were made for two jet pressure ratios, corresponding to ideally expanded ($P_e/P_a \cong 1$) and highly underexpanded ($P_{oj}/P_a = 6$, $P_e/P_a = 3.17$). The test setup for the single underexpanded jet was the same, except that the multijet centerbody in the tunnel was replaced with a convergent nozzle of exit diameter $D = 30$ mm. The axial extent of the imaging was $x = 5D$.

C. BOS Experimental Procedure

The procedure used for the BOS technique was essentially the same for the multijet and axisymmetric jet flow studies.

A structured background to focus on was created by means of a normal random number generator. This generated a 2000×2000 matrix of random numbers the elements of which were normally distributed with zero mean, unit variance, and standard deviation. The matrix was plotted as a binary image, by using black dots for all

nonzero values. Because tunnel vibrations could cause erroneous results on cross-correlation, care was taken to minimize vibrations of the background and camera. The printed-out pattern was sandwiched between two thin sheets of glass and mounted on a heavy stand fixed on a concrete block to minimize vibrations (see Fig. 2).

The background was illuminated to achieve a better signal-to-noise ratio by means of placing a large halogen lamp far enough behind so as to approximate parallel beam conditions, thus eliminating the need for methods to resort sets of fan beam projections into parallel beam projections.[11] The imaging was taken through the schlieren windows of the tunnel. The optimal locations for the background, light source, and camera were arrived at by using the methodology outlined in Ref. 9 and keeping in mind that increasing sensitivity (displacement of image) meant lower physical resolution because the interrogation size used in the correlation algorithm would have to be correspondingly larger.

The images were captured using a commercially available Sony DSC F-707 digital still camera with 5.1-megapixel resolution. The exposure time was limited to 1/2500th of a second to enable sufficient depth of field to focus on the flow as well as the background. The camera was mounted on a heavy tripod, fixed to the ground 0.7 m away from the tunnel.

As pointed out before, the multijet experiment required at least two views, whereas a single was sufficient for an axisymmetric jet. The multijet flow was imaged at $\theta = 0$ deg (section *AA*) and 45 deg (section *BB*) with 0 deg coincident with the $z = 0$ axis. This was achieved by rotation of the nozzle assembly. In the case of the axisymmetric jet, the flow was imaged at $\theta = 0$ deg (see Fig. 3b for coordinate system). For each case, three images were captured and the displacement fields were averaged. As is obvious for the cruciform configuration chosen, a perspective at any angle beyond 45 deg would yield images identical to those already obtained. The exposure time of the imaging was limited by the camera (0.4 ms). Due to the inherent unsteadiness (of the order of 5–7 kHz) present in such turbulent flows, slight blurring of the edges of the shear layer and the shocks is unavoidable because of the low shutter speed (4×10^{-4} s) compared to the time scale of the jet, which results in inherent averaging. Because of the problems in imaging at very high shutter speeds of above 10 kHz (required to resolve the turbulent shear layers at 5–7 kHz), a better solution would be to use a high-power short-duration flash to illuminate the background. However, the focus of this work was not to capture the instantaneous density field in the shear layers but rather to obtain a mean picture. Hence, the exposure time used here is satisfactory.

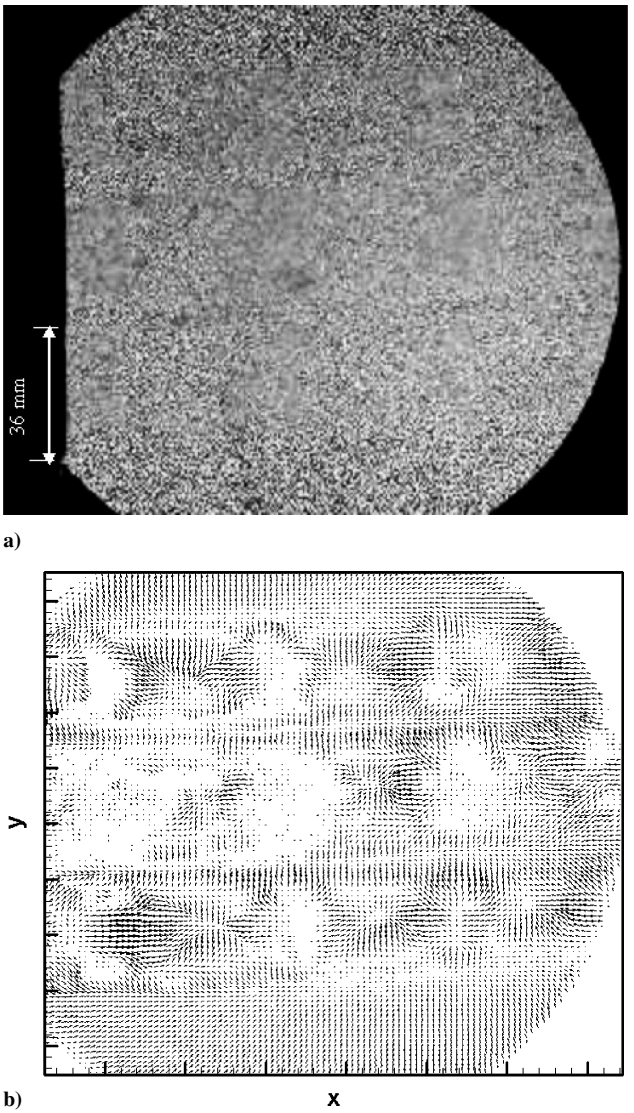

Fig. 4 Background imaged though multijet flow at view angle $\theta = 0$ deg: a) background dot pattern at 0 deg and b) corresponding displacement (density gradient) field.

IV. Results and Discussion

A. Validation of Tomographic Technique

1. Validation of Extraction of Central Plane on Multijet Flows

Figure 4a shows the background dot pattern at $\theta = 0$ deg for the four-jet case. Because of the cruciform configuration, three jets are visible along the line of sight with the center jet being an integrated effect of the one diametrically opposite to it. The blurring of the dots in the vicinity of the shear layers and the shocks is caused by inadequate imaging speed compared to the shock unsteadiness and turbulence of the shear layers. The cross-correlation algorithm blanks out the corresponding mesh points. These are later interpolated from the neighboring mesh points. Although this results in a loss of resolution, it does not result in an erroneous conclusion (as is seen by observation presented later, where the shear layer is clearly demarcated again). Figure 4b shows the displacement field calculated from cross-correlation of the images under no-flow and flow conditions. The cross-correlation was carried out on a 200×200 grid fitted to the image. The top and bottom jets are seen as well as the integrated effect of the other two at the $\theta = 0$ deg (section *AA*) plane. The background dot pattern imaged at $\theta = 45$ deg (section *BB*) is very similar except in jet spacing and, hence, has not been reproduced here.

As pointed out earlier, the displacements obtained through cross-correlation are the gradients of the density field. The derivative of the density gradients forms an elliptic partial differential equation also commonly known as the Poisson equation (see Ref. 9 for details). Neumann boundary conditions are chosen in which a normal derivative is specified at the boundaries. To fix the integration constant, it is required to peg the density value to a known (reference) value in the flowfield. This point is chosen to be the jet exit and, thus, the method performs well when the density is predicted correctly elsewhere in the flow and in the ambient (see Ref. 9 for details). The setup geometry and lens parameters are used to effect the unit conversion. This is then solved on the same rectangular grid and yields the line-of-sight integrated density field as seen in Fig. 5. This procedure is repeated for the data obtained from imaging at $\theta = 45$ deg. These two density fields then form the input projected data set for the filtered backprojection. The same procedure has been adopted for the axisymmetric sonic jet as well, excepting that a single data set ($\theta = 0$ deg) is sufficient.

Figure 5 corresponds to one of the two ($\theta = 0$ deg) projected data sets as input to the tomographic algorithm. The density contour lines show the two jets in the centerplane (section *AA*) clearly. At the center, the field is not so clear due to the integrating effect of the other two jets on either side. Furthermore, the "center jet" also appears larger as it is slightly out of focus. No attempt has been made to filter out the noise from the entire region to avoid artifacts generated by the filtering process. However, the signal-to-noise ratio in the regions of interest is adequate for drawing unambiguous conclusions.

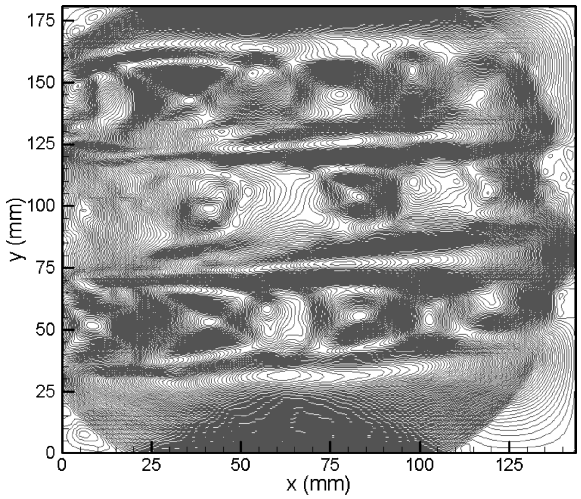

Fig. 5 Projected (line-of-sight integrated) density field as computed from the Poisson equation.

Figure 6a shows the backprojected normalized density field at the central plane. Only the two jets in the central vertical plane with exit jet diameters of about 36 mm and separation of about 20 mm are visible. This shows that the extraction of the central plane using tomography has been successfully achieved. Furthermore, the grayscale mapped to the density shows the expected distribution, as also seen in Fig. 6b, which shows the variation of centerline density for the lower of the two identical jets. The value from isentropic relations at the nozzle exit is also indicated. The bright spots are due to the density rise at the intersection of the shocks at the end of the shock cells and would have been seen again a couple of shock cells downstream had the imaging extended farther downstream. This is also seen in the single axisymmetric underexpanded jet, which will be presented in the next section. Figure 6c shows the density extracted along section *CC* (parallel to *AA* but passing through the jet nearest the camera). Although the extraction of the plane is achieved, the picture shows considerable noise. Hence, although the extraction of the desired planes has been achieved, the resolution of Figs. 6a and 6c would be better with two improvements. First, improved imaging speed would reduce not only the blurring and subsequent interpolation but also the background noise. Second, only two perspectives have been chosen between the angles 0 and 45 deg. This decreases the resolution of the nondiametral sections (e.g., *CC*). However, only two perspectives were chosen due to the fact that in a noisy environment (due to small vibrations of the background) multiple perspectives would only result in increasing the noise, thus negating any improved resolution. However, with increased imaging speed, the noise would reduce and increased perspectives would improve the resolution of the shock cells and shear layers.

2. *Validation of Density on Ideally Expanded Sonic Jet*

The results from application of BOS on the ideally expanded sonic jet are first presented and compared with the centerline density variations, which were calculated from pitot measurements using isentropic relations. The density gradients are increasingly pronounced with increase in degree of underexpansion. For moderately underexpanded cases, the density gradients become weaker and the sensitivity of the system has to be increased,[9] thereby also amplifying the sources of noise in the background. For ideally expanded cases, care has to be taken to ensure that slight vibrations or noise in the imaging do not manifest as density gradients.

Figure 7a shows the comparison of the centerline density (normalized by ρ_a) variation from BOS and through calculation from pitot probe measurement on the same setup for the ideally expanded sonic jet. As expected, the density normalized by the ambient remains very close to unity from the nozzle exit downstream, and the two measurements exhibit excellent agreement. The slight mismatch at the exit (of the order of 1%) is due to the fact that the pitot measurements were made from a different run. However, the drop (~99% of exit value) at $x = 5D$ in each case is comparable. Figure 7b, which shows a plot of the radial variation of jet density normalized by ambient value across the jet at $x/D = 1$, shows uniform distribution of density as expected for this case. The BOS is now applied to a highly underexpanded supersonic jet to extract the density field.

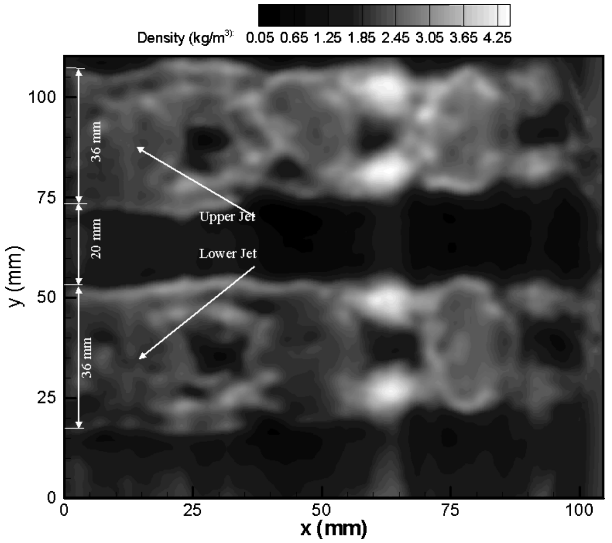

Fig. 6a Backprojected density field in the central plane of the four-jet configuration.

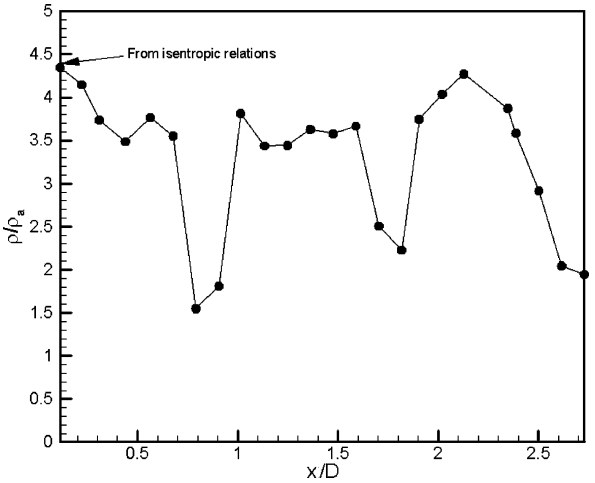

Fig. 6b Variation of centerline density for lower jet of four-jet configuration.

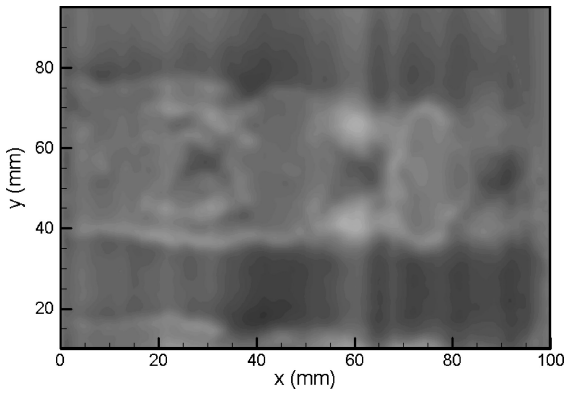

Fig. 6c Plane passing through front jet: cross section *CC*.

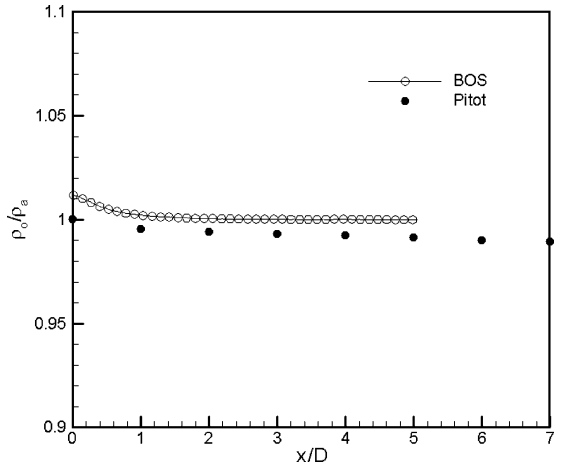

Fig. 7a Axial variation of centerline density in ideally expanded jet.

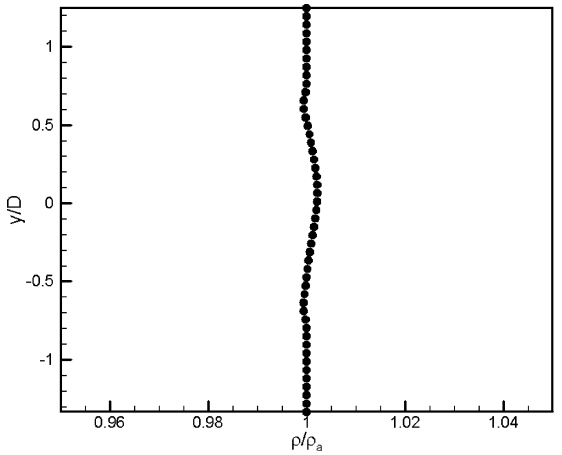

Fig. 7b Radial variation of density at $x/D = 1$ in ideally expanded jet.

B. Results on the Underexpanded Jet

Figure 8a shows the integrated density gradient (displacement) vector field for the same case. This was obtained from a cross-correlation algorithm whose interrogation size was set at 24×24 pixels in size. The vectors point to regions of decreasing density. This corresponds to bidirectional schlieren. The characteristic features of highly underexpanded supersonic jets are observed in the figure. Figure 8b is a contour plot of jet density in the central plane of the jet over a streamwise extent of $4.3D$. Because the flow is underexpanded, expansion waves and an internal weak shock system appear in the flow. Thus, there is Mach wave radiation corresponding to the structures moving at supersonic velocity in the shear layer. This shows that the structures traveling in the shear layer as well as the Mach waves have been picked up, hence demonstrating the sensitivity of the system. It can be observed that the ambient density is well represented in the plot. Figure 8c plots the variation of normalized centerline density with axial distance. As is characteristic of underexpanded jets, the pressure oscillation in the flow begins with a smooth expansion from the sonic value at the exit (indicated in the plot) followed by recompression toward the first pressure peak in two stages. This corresponds to a sharp decrease in the density from the value at nozzle exit ($\rho_e/\rho_a = 3.32$ from isentropic relations) to a minimum at $x/D \sim 0.5$, followed by an increase to almost the exit value. Thereafter, the density oscillation continues over the imaged region up to $x/D \sim 4$. This corresponds to the shock system seen in the conventional schlieren for the same case. The mean ρ_e/ρ_a over this region is seen to be unity, as should be the case. The increase of density over the Mach disk is not instantaneous but occurs across a region because of the finite size of the interrogation region in the correlation algorithm and the finite time duration of the exposure. Reductions in both of these would lead to sharper density images and higher resolution in the regions of the shock.

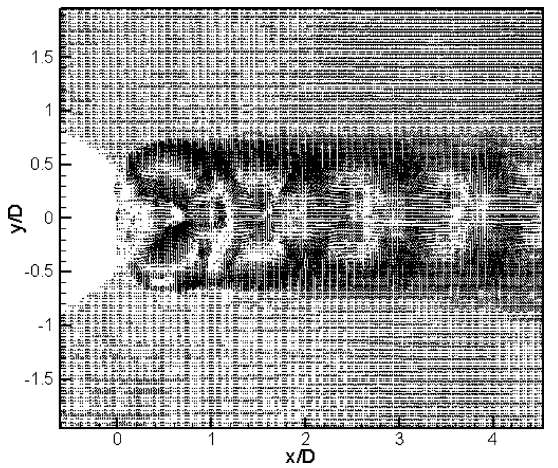

Fig. 8a Vector field of density gradients in the underexpanded jet ($P_e/P_a = 3.17$) obtained from cross correlation.

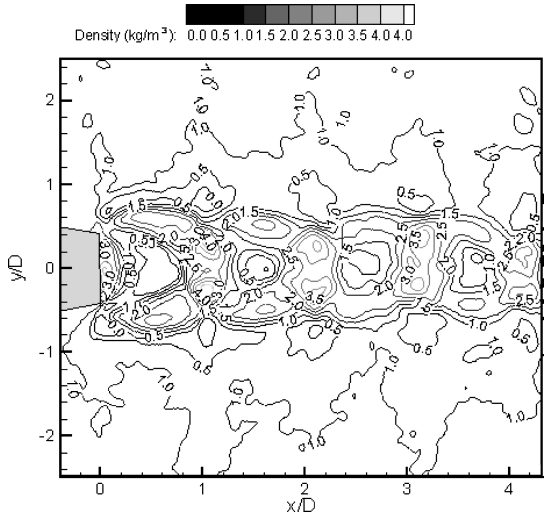

Fig. 8b Density contours in the underexpanded jet ($P_e/P_a = 3.17$) using BOS.

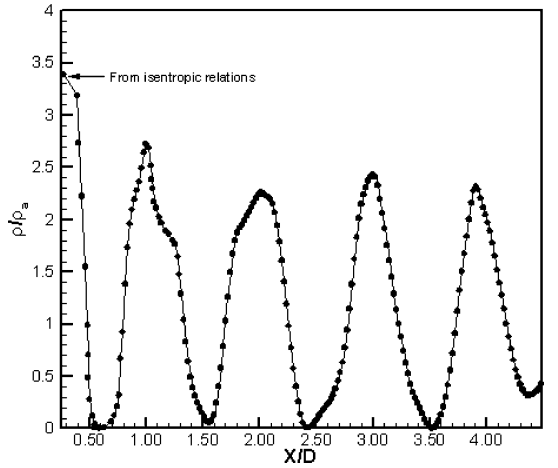

Fig. 8c Axial variation of normalized centerline density for underexpanded jet ($P_e/P_a = 3.17$).

Figure 9 shows typical features of a highly underexpanded jet. The main features of the flow are evident, as is the consistency with the results just presented. Figure 10a shows the conventional schlieren of the jet ($P_{oj}/P_a = 6$, $P_e/P_a = 3.17$) with the knife edge in the horizontal position implying that density gradients in the vertical plane ($\partial\rho/\partial y$) are obtained. Although BOS yields the

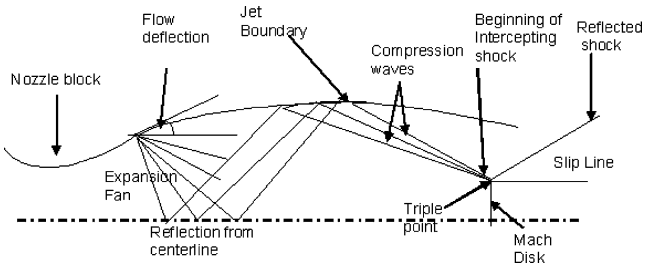

Fig. 9 Schematic of typical features in a highly underexpanded jet.

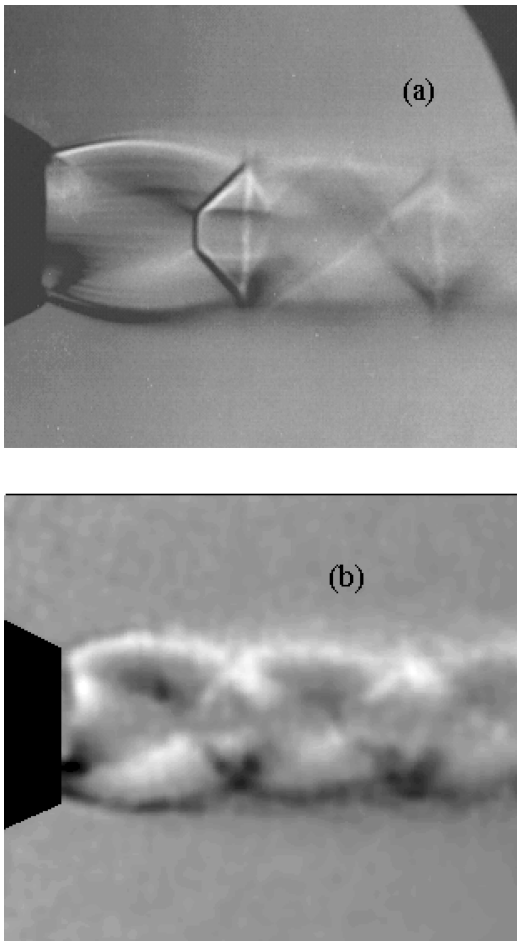

Fig. 10 Underexpanded jet at $P_{oj}/P_a = 6$: a) conventional schlieren (horizontal knife edge) and b) corresponding density gradient field from BOS.

density gradients in both directions, only the corresponding field $(\partial\rho/\partial y)$ in the central plane is shown here (Fig. 10b) for comparison. The qualitative features of the shocks are identical in both images.

V. Conclusions

The BOS technique has been successfully applied to determine the mean density field of an underexpanded sonic jet for the first time. This effort involved two major steps:

1) The FBPT technique validation was successfully carried out using a multijet configuration. Two view angles were used to obtain the central plane of the configuration. The results show that the technique is capable of obtaining a desired plane of interest from a line-of-sight integrated data set.

2) Comparison of the density field of an ideally expanded jet obtained with BOS exhibited good agreement with pitot data and was thereafter applied to a highly underexpanded sonic jet to obtain density contours.

The obtained density field shows all of the familiar features of an underexpanded jet, such as the curved shock at the lip and internal weak shock system. However, the high unsteadiness of the jet resulted in a slight averaging at the current sample rate. Shorter exposure times, brought about by either increasing shutter speed or reducing illumination pulse width, can successfully address the problem. Furthermore, the results are less prone to noise for flows with large density gradients. However, this study shows that meaningful quantitative density data can be extracted by using minimal hardware with this methodology.

Acknowledgments

This work was supported by Aeronautical Research and Development Board Grant DARO/08/1031170/2001. The author acknowledges the encouragement of P. R. Viswanath, Head of the Experimental Aerodynamic Division, National Aerospace Laboratory (NAL), and his insightful comments on the results and the support of N. B. Mathur for the experiments. The technical support of the NAL Base Flow facility staff during the imaging is acknowledged. The author thanks the anonymous referees who helped to improve the clarity of the text.

References

[1]Meier, G. E. A., "New Optical Tools for Fluid Mechanics," *Proceedings of the 8th International Symposium on Flow Visualization* [CD-ROM], Sorrento, 1999, Paper 226.

[2]Meier, G. E. A., "Computerized Background Oriented Schlieren," *Experiments in Fluids*, Vol. 33, No. 1, 2002, pp. 181–187.

[3]Raffel, M., Richard, H., and Meier, G. E. A., "On the Applicability of Background Oriented Optical Tomography for Large Scale Aerodynamic Investigations," *Experiments in Fluids*, Vol. 28, No. 6, 2000, pp. 477–481.

[4]Richard, H., Raffel, M., Rein, M., Kompenhans, J., and Meier, G. E. A., "Demonstration of the Applicability of a Background Oriented Schlieren (BOS) Method," *Selected Papers from the 10th International Symposium on Applications of Laser Techniques to Fluid Mechanics*, Springer, Berlin, 2002.

[5]Dalziel, S. B., Hughes, G. O., and Sutherland, B. R., "Synthetic Schlieren," *Proceedings of the 8th International Symposium on Flow Visualization* [CD-ROM], Sorrento, Italy, 1998.

[6]Dalziel, S. B., Hughes, G. O., and Sutherland, B. R., "Whole Field Density Measurements by 'Synthetic Schlieren'," *Experiments in Fluids*, Vol. 28, No. 4, 2000, pp. 322–335.

[7]Sutherland, B. R., Dalziel, S. B., Hughes, G. O., and Linden, P. F., "Visualization and Measurement of Internal Gravity Waves by 'Synthetic Schlieren.' Part I. Vertically Oscillating Cylinder," *Journal of Fluid Mechanics*, Vol. 390, 1999, pp. 93–126.

[8]Onu, K., Flynn, M. R., and Sutherland, B. R., "Schlieren Measurement of Axisymmetric Wave Amplitudes," *Experiments in Fluids*, Vol. 35, No. 1, 2003, pp. 24–31.

[9]Venkatakrishnan, L., and Meier, G. E. A., "Density Measurements Using Background Oriented Schlieren Technique," *Experiments in Fluids*, Vol. 37, No. 2, 2004, pp. 237–247.

[10]Sims, J. L., "Tables for Supersonic Flow Around Right Circular Cones at Zero Angle of Attack," NASA SP-3004, 1964.

[11]Kak, A. C., and Slaney, M., *Principles of Computerized Tomographic Imaging*, IEEE Press, New York, 1988.

[12]Mathur, N. B., Ramesh, R., and Ramesh, G., "Calibration Studies in the High Speed Base Flow Wind Tunnel," National Aerospace Lab., PD EA 9804, Bangalore, India, 1998.

[13]Mathur, N. B., and Kumar, R., "A Novel Technique for the Direct Measurement of Afterbody Drag in the Presence of Multi Jet Nozzle Exhausts," AIAA Paper 2003-1196, Aug. 2003.

R. Lucht
Associate Editor